



## Laser-joined $\text{Al}_2\text{O}_3$ and $\text{ZrO}_2$ ceramics for high-temperature applications

Floriana-Dana Börner\*, Wolfgang Lippmann, Antonio Hurtado

Dresden University of Technology (TU Dresden), Institute of Power Engineering, Chair of Hydrogen Technology and Nuclear Power Engineering, George-Bähr-Str. 3, D-01062 Dresden, Germany

### ARTICLE INFO

#### Article history:

Received 2 November 2009

Accepted 10 July 2010

### ABSTRACT

A laser process is presented that has been specially developed for joining oxide ceramics such as zirconium oxide ( $\text{ZrO}_2$ ) and aluminium oxide ( $\text{Al}_2\text{O}_3$ ). It details, by way of example, the design of the laser process applied for to producing both  $\text{Al}_2\text{O}_3$ – $\text{Al}_2\text{O}_3$  and  $\text{ZrO}_2$ – $\text{ZrO}_2$  joints using siliceous glasses as fillers.

The heat source used was a continuous wave diode laser with a wavelength range of 808–1010 nm. Glasses of the  $\text{SiO}_2$ – $\text{Al}_2\text{O}_3$ – $\text{B}_2\text{O}_3$ –MeO system were developed as high-temperature resistant brazing fillers whose expansion coefficients, in particular, were optimally adapted to those of the ceramics to be joined. Specially designed measuring devices help to determine both the temperature-dependent emission coefficients and the synchronously determined proportions of reflection and transmission.

The glass–ceramic joints produced are free from gas inclusions and macroscopic defects and exhibit a homogenous structure. The average strength values achieved were 158 MPa for the  $\text{Al}_2\text{O}_3$  system and 190 MPa for the  $\text{ZrO}_2$  system, respectively.

© 2010 Elsevier B.V. All rights reserved.

### 1. Introduction

Owing to their excellent properties in the high-temperature range, ceramic materials are an indispensable group of materials for various future reactor designs. They are unrivalled, in particular, in the numerous high-temperature and very high-temperature reactor (V)HTR applications. Taking into consideration the innovative energy conversion processes that become accessible through high-temperature reactors, it is evident that ceramic materials will play a key role in the future. One example is the implementation of hydrogen-based power systems that make use of thermochemical hydrogen generation to provide large quantities of hydrogen at low cost. The favoured nuclear-heated iodine–sulphur process requires operating temperatures of at least 900 °C in the sulphuric acid cycle in order to achieve a total efficiency level of more than 50% [1–3]. With safety margins to be observed, temperatures of not less than 1200 °C, partly in aggressive atmospheres, must be made safely manageable by means of materials engineering. Traditional metallic materials cannot fulfil these requirements. National and international research efforts [3,4] are therefore intensively focused on finding suitable materials or material systems. Ceramic materials, both constructional and functional, are the preferred group of materials. To be able to produce technologically relevant assemblies, suitable application-specific joining technologies need to be developed for the selected

materials. Well-established welding processes for metallic materials are generally inappropriate for ceramic components. Preliminary investigations [5] have shown that, besides conventional joining processes in a furnace atmosphere [6], laser brazing can be successfully used for the production of the high-temperature resistant joints in ceramic materials.

Experimental selection processes have shown that a diode laser beam in the wavelength range of 808–1010 nm is very well-suited for joining both non-oxide and oxide ceramics [7]. The brazing fillers used can be oxidic glass systems whose thermochemical and physical properties have been modified to match the relevant requirement profiles of the ceramics to be joined [5,7–13,21].

Laser radiation is an energy source that is particularly suited for melting the brazing filler in the joining zone. It enables localized heating of the joining zone without the complete assembly having to be heated to joining temperature. Process times are thus considerably shorter, and the combining of low-melting materials with the ceramic can also be achieved without damage to the materials during the joining process. Furthermore, there are no component size restrictions imposed by the internal dimensions of a sintering furnace. A characteristic result of the short process times is further that the glass–ceramic joint is achieved without intermediate layers – a fundamental difference to processes aimed at producing a functional interlayer (with or without metallic components) [6,14,15].

The laser joining process presented in this article, which uses high-temperature resistant oxidic brazing fillers, is a suitable technology for joining ceramic components also in series production. The article briefly describes the characteristic features of this laser technology as well as the specific material properties of the brazing filler systems for oxide ceramics.

\* Corresponding author.

E-mail addresses: [floriana.boerner@tu-dresden.de](mailto:floriana.boerner@tu-dresden.de) (F.-D. Börner), [wolfgang.lippmann@tu-dresden.de](mailto:wolfgang.lippmann@tu-dresden.de) (W. Lippmann), [antonio.hurtado@tu-dresden.de](mailto:antonio.hurtado@tu-dresden.de) (A. Hurtado).

Polycrystalline  $\text{Al}_2\text{O}_3$  and  $\text{ZrO}_2$  ceramics have excellent high-temperature properties and have been tried and tested in various technological applications. In order to open up new fields of application beyond the existing ones, it is often necessary to produce more complex geometries using high-temperature-resistant joints. Due to the semi-transparency of the investigated oxide ceramics in the laser wavelength range used and the involved release of heat in the volume of the components, it is crucial for process implementation to understand the optical properties characteristic of the material.

Due to its capability of transporting oxygen selectively over defects, yttrium-stabilized  $\text{ZrO}_2$  is the material used for oxygen sensors;  $\text{Al}_2\text{O}_3$  with its low electrical conductivity is used as insulation material. These materials can be combined, e.g. for the production of high-temperature resistant oxygen sensors [5,7,11,12]. If other ceramics, e.g. electrically conductive ones, are also included, various functional applications are conceivable.

For instance, temperature sensors or thermoelectrical generators can be constructed for the autonomous power supply of measuring systems. The development of such systems is a direct contribution to increasing the safety of nuclear installations.

## 2. Materials and methods

### 2.1. Materials

The experiments presented here were conducted with a laser joining technology optimized for two  $\text{Al}_2\text{O}_3$  ceramics (AL23, Friatec AG/Mannheim and RK87T, CeramTec AG/Plochingen) and one  $\text{ZrO}_2$  ceramic (FZY, Friatec AG). All ceramics were provided as solid round rods with diameters of 6 mm and 4 mm for the  $\text{ZrO}_2$  of Friatec GmbH, respectively. The parts to be joined were pressed into shape. The surface properties obtained after sintering were not modified by any additional processing (“as fired” quality).

The glass filler used was from the system  $\text{SiO}_2\text{--MeO--Me}_2\text{O}_3$  ( $\text{Me}^{2+}$ : Ba, Sr;  $\text{Me}^{3+}$ : B, Al, La). All joining experiments conducted so far have demonstrated that this filler is very well-suited for both  $\text{Al}_2\text{O}_3$  and  $\text{ZrO}_2$  ceramic qualities under test.

The main steps for filler production are: mixing and homogenization of the weighed raw materials with ethanol into a paste, removal of the added alcohol at 80 °C and subsequent melting of the mixture in the lab chamber furnace at 1250 °C. After refining, the molten glass is poured out from the crucible and at the same time quenched. The resulting pieces of glass are coarsely crushed and subsequently finely ground to grain sizes smaller than 63  $\mu\text{m}$ .

### 2.2. Methods

#### 2.2.1. Determining emissivity ( $\epsilon$ ) of the ceramic

Process control requires the knowledge of the instationary temperature field in the area of the joining seam. For technological reasons, the temperature can only be determined at the ceramic surface using an optical measuring method. Optical measuring methods require that the temperature-dependent emissivity of the ceramic is known. Emissivity defines how much radiation the real body surface emits as compared with an ideal blackbody radiator. This is based on the physical phenomenon that all bodies with temperatures above absolute zero (0 K or  $-273.15$  °C) emit electromagnetic radiation. However, the thermographically obtained temperature fields characterize only the surface temperature of the body, but give no information about the temperature distribution inside the body [16].

In this specific case the temperature was measured using a bolometric infrared camera (“VarioCAM” from InfraTec GmbH, Germany). The measuring range of this camera is between  $\lambda = 7.5$  and 14.5  $\mu\text{m}$ . In order to protect the camera sensor from the intensive laser radiation and to avoid erroneous measurements, an optical filter is built into the optical path of the camera, selectively filtering out the wavelength range of the laser radiation. The camera system including the laser filter was calibrated with a black radiator prior to the experiments. The shots of the infrared camera were recorded at a preselected emission coefficient of  $\epsilon = 1$ . To determine a sufficiently exact temperature from the recorded values, this value is corrected by a spectral emission coefficient separately obtained for each ceramic under investigation and relevant to the camera used (instrument-specific emission coefficient).

This emission coefficient is determined with the aid of an electrically heated small furnace whose core component is a silver bath with the necessary peripherals, as shown in the experimental set-up (Fig. 1, left).

The ceramic specimen to be investigated is placed on the surface of the silver bath and heated to 1100 °C at a constant heating rate. The ceramic surface carries a metal platelet of e.g. silver or gold. Through the deformation of the platelet due to solid–liquid phase transition, the exactly defined melting temperature of the metal used ( $T_{\text{Ag}} = 960.5$  °C,  $T_{\text{Au}} = 1063$  °C) (Fig. 1, right) can be optically captured. By adjusting the temperature measured by the camera to the surface temperature thus determined, it is possible to determine the emission coefficient specific to the measuring device.

When the standard materials are selected, care must be taken to avoid reactions between the ceramic and the metal selected. The specimen height should also be selected such that the temperature

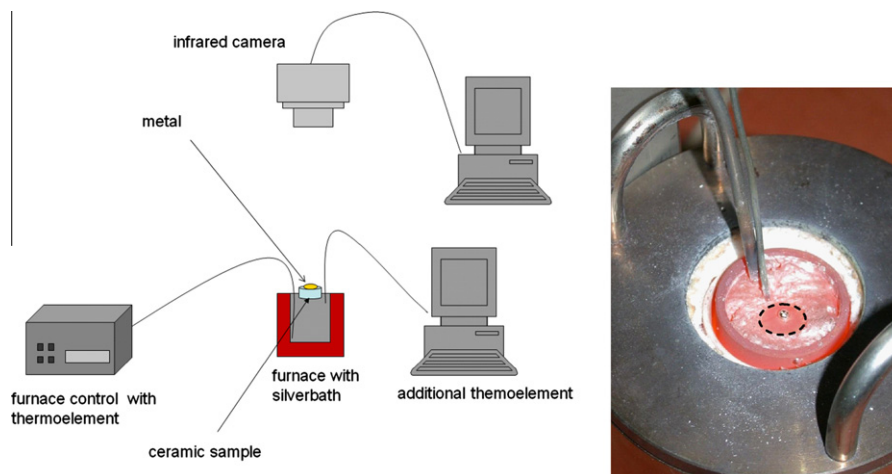


Fig. 1. Left: experimental set-up to determine emissivity of ceramics at high-temperatures right: ceramic surface with silver sphere on the surface.

difference between the lower contact area of the tablet on the silver bath and the upper area to be measured is kept to a minimum. Preliminary measurements showed that, in the operating range of the infrared camera, the measurement results are not affected by the radiation transmitted by the ceramic specimen from the silver bath.

### 2.2.2. Transmission, reflection and absorption of ceramics

Laser materials processing technology requires that the materials are able to absorb the irradiated energy at the wavelengths used. Exposure to laser radiation causes laser–material interactions which are influenced by various factors. Variables that influence the laser process are material characteristics such as material structure, size and distribution of pores, proportion of crystalline phase, surface quality, material purity and the type of contaminants present [20–22]. These influence the reflection ( $R$ ) and, as a characteristic of oxide ceramics, the transmission ( $T$ ) of the laser beam through the irradiated body [18,19]. The following equation represents the mathematical relation between the optical properties of a material:

$$R + T + A = 100\%$$

In distinction from the investigations conducted so far on this subject [17,20–22], which were based on methods such as photo-thermal interference measurement, integral reflectometer measurement or laser calorimetry and alternatively determined either the reflection, transmission or absorption of ceramics directly, a device for synchronous measurements of reflection and transmission has been implemented at the TU Dresden (GigaHertz Optik GmbH, Germany). This measuring method is based on the assumption that the laser beam emitted by a laser diode penetrates the ceramic specimen at a defined angle perpendicular to the surface normal. An Ulbricht sphere is located above the specimen to capture the total radiation which is reflected directly and diffusely. The proportion of this radiation in relation to the total radiated optical flux can be captured with a photodetector. A special additional sensor allows the directly reflected proportion of the radiation to be captured. A second Ulbricht sphere is located below the specimen. It captures the total transmitted proportion of the radiation. Here again, a second sensor in a special configuration allows capture of the directly transmitted proportion of the radiation (see Fig. 2).

Subsequently to the measurements, both the direct and the diffuse proportion of reflection and transmission are output separately, and the absorption of the investigated ceramics is calculated as the difference from 100%. The measurement laser used is a laser diode with a wavelength of 808 nm or 940 nm

and 60 mW laser power. When the general conditions are observed, this system can be used to conduct measurements on specimens at temperatures of up to approx. 900 °C.

### 2.2.3. Laser-induced joining

Due to their low thermal conductivity of <30 W/m K and their coefficients of thermal expansion of  $>8.5 \times 10^{-6} \text{ K}^{-1}$ , both  $\text{Al}_2\text{O}_3$  and  $\text{ZrO}_2$  are sensitive to thermal shocks. That is, heating up of a component with a laser beam that is largely absorbed at the component surface would not be feasible within process times relevant to manufacture. However, since these ceramics are semi-transparent to the wavelengths of the diode laser radiation used here (808–1010 nm), it is possible to heat oxide ceramic components in the volume of the joining zone by optimally guiding the laser beam [5]. The thermally induced stress in the material can thereby be kept to such a minimum that damage to the material structure can be prevented. It has proved advantageous to rotate the components to be joined under the laser beam and thus to achieve uniform heating of the volumetric joining zone. Besides laser power, focus position as well as beam duration are the laser parameters to be optimized for the process. The brazing fillers are essentially optimized by their composition, which can be varied to influence the coefficient of thermal expansion, liquid temperature, wettability and laser absorption.

The radiation source used was a diode laser “Rofin DL 031 Q” (ROFIN-SINAR Laser GmbH) with a maximum beam power of 3.1 kW (continuous wave at 808 nm and 940 nm) and a diode laser Laserline LDS 1500–10000 from Laserline GmbH with a beam power of 10.1 kW (continuous wave, wavelengths 915 nm, 940 nm, 980 nm and 1030 nm).

The example selected in this case was processed with the 3.1 kW laser with a fixed optical unit and a focal length  $f = 305 \text{ mm}$ . The geometry of the laser beam on the irradiated joining area was a circle of 6.3 mm diameter. The laser beam was positioned on the specimen surface in such a way that the joining seam was always centred in the laser spot.

The ceramic parts to be joined were each fixed in a chucking device on one side and synchronously rotated during the joining process (Fig. 3). The rotational speed was approx. 1 rev/s and the irradiation area was symmetrically positioned in relation to the joining zone it heated. By rotation it was possible to heat the joining zone uniformly on its entire perimeter.

In this case, the  $\text{Al}_2\text{O}_3$  or  $\text{ZrO}_2$  ceramics are joined using glass fillers which recrystallize to a certain proportion during the cool-down phase. Suitable fillers are selected according to different criteria such as the material parameters of the partners to be joined, the future application temperature of the joined component and

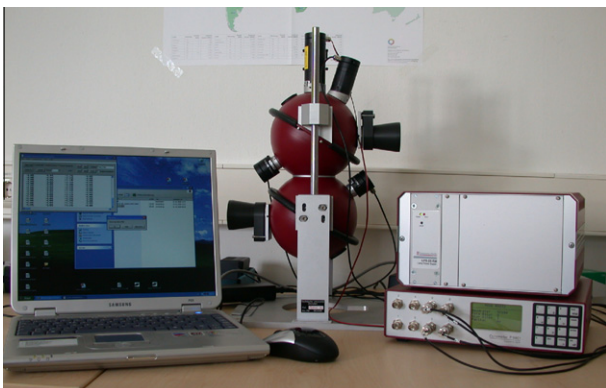


Fig. 2. Dual Ulbricht spheres for synchronous measurement of transmission and reflection.

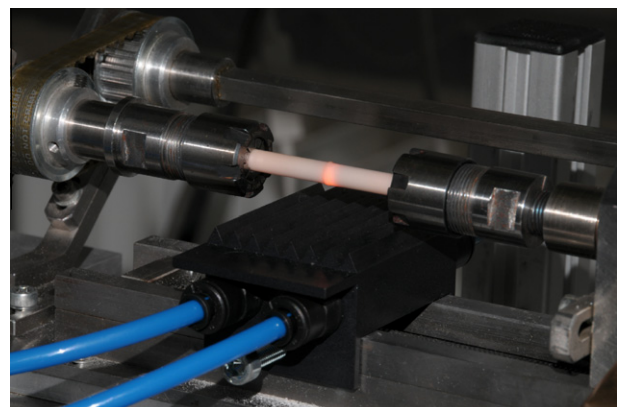


Fig. 3. Chucking and rotating device for laser joining.

**Table 1**  
Glass filler systems for laser joining of Al<sub>2</sub>O<sub>3</sub>.

Filler	Oxidic composition <sup>a</sup>										T <sub>A</sub> (°C)	T <sub>B</sub> (°C)	T <sub>C</sub> (°C)
	SiO <sub>2</sub>	ZrO <sub>2</sub>	BaO	CaO	MgO	SrO	ZnO	Al <sub>2</sub> O <sub>3</sub>	B <sub>2</sub> O <sub>3</sub>	La <sub>2</sub> O <sub>3</sub>			
Filler 1	█		█		█				█		746	1003	1045
Filler 2	█		█		█		█	█	█		707	824	1007
Filler 3			█			█		█	█		751	913	1030
Filler 4	█		█		█		█		█		692	668	842
Filler 5	█		█		█						818	1108	1123
Filler 6	█		█		█						881	1088	1151

<sup>a</sup> Blue < 50%; red < 40%; yellow < 30%; green < 20%; grey < 10%.

the composition of the ambient atmosphere during use. The following table lists some glass systems suited for applications using the Al<sub>2</sub>O<sub>3</sub> system [13]. The defined compositions of high-temperature fillers (fillers 1–6) are given as examples with their softening (T<sub>A</sub>), half ball (T<sub>B</sub>) and flow (T<sub>C</sub>) temperatures: (see Table 1).<sup>1</sup>

It is of utmost importance for the joining process to match the expansion coefficient of the glass filler to that of the ceramic. Only minimal differences can ensure that mechanical stress will not lead to joint failure during cooling or in the long term. Such stress is only partly remedied by an additional thermal treatment of the joined components in the furnace, which supports slow relaxation of induced stress above the T<sub>g</sub> temperature of the glass [9].

The filler was applied in a thin layer on the surface to be joined of one or both ceramics. Low pressure is applied to press the parts to be joined to each other so that the filler is locally fixed in the joining gap without quantity losses until the melting temperature of the filler is reached. Frequently, the glass phase on the ceramic is now pre-sintered in a furnace process to ensure better filler adhesion. However, this means adding a further technological step to the overall joining technology [12] to the detriment of process optimization.

Four-point bending strength testing was performed to evaluate the strength of the produced joints. The specimens were tested following the DIN-EN 843-1 standard at room temperature. The test configuration had a 40 mm centre-to-centre support roller span and a 20 mm centre-to-centre load roller span. The selected test velocity of 0.5 mm/min allowed breakage of the test specimen within 20–25 s. The specimens had a cylindrical geometry and were 6 mm in diameter.

### 3. Results and discussion

#### 3.1. Determining emissivity ( $\epsilon$ ) of the ceramic

Fig. 4 shows how the solid–liquid transition of the reference material (here: silver) was determined graphically and the assigned reference temperature was selected for determining the emission coefficient of the ceramic surface. When interpreting the measurement results, it should be noted that ceramic and silver have different emission coefficients. This, however, has not been taken into account in the graphical representation (set emission coefficient  $\epsilon = 1$  for all materials).

The measurements conducted on an “as fired” surface and subsequent calculations yielded an emissivity  $\epsilon$  of 0.73 for the Al<sub>2</sub>O<sub>3</sub> ceramic and of 0.81 for the ZrO<sub>2</sub> ceramic around the melting temperature of silver. Four samples of each were measured and the mean obtained from at least two individual points on the ceramic

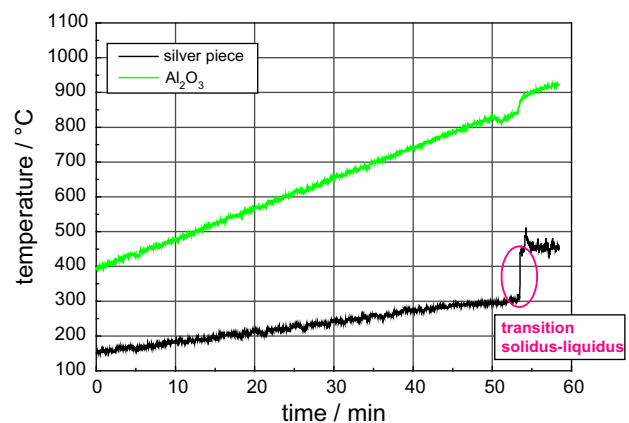


**Fig. 4.** Graphical representation to establish the real reference temperature for the determination of the emission coefficient.

surface was calculated. These emission values were entered into the software “IRBIS online 2.2” of the infrared camera for correction of the temperature output by the infrared camera.

#### 3.2. Laser-induced joining

Knowledge of the heating behaviour of the ceramics and the glass filler is an important requirement for conducting and optimizing the laser joining process. Investigations on the heating rates of the ceramic achieved in the joining zone with or without the brazing filler at constant laser power showed that the joining zone with filler heats up faster than the ceramic base material due to the higher absorption of laser radiation in the filler.

Since ZrO<sub>2</sub> has a higher absorption coefficient for diode laser radiation than Al<sub>2</sub>O<sub>3</sub>, a more significant effect of the filler on heating behaviour is seen for Al<sub>2</sub>O<sub>3</sub> than for ZrO<sub>2</sub>.

The number of structural defects in the ceramics increases with temperature, and as a result, the absorption of the diode laser radiation in the ceramic is also intensified. Since different temperature-dependent structural defect mechanisms are involved, a linear increase of absorptivity cannot be expected. This is clearly demonstrated in the heating curves shown in Fig. 5 for different samples of Al<sub>2</sub>O<sub>3</sub> ceramics. At constant laser power, the temperature gradient changes significantly and reproducibly in several stages.

In the real joining process the effect of the brazing filler in the joining zone should additionally be considered. Since, in general, the filler has a higher absorption coefficient for diode laser radiation than the ceramic, a joining seam with filler is heated more intensively than the base ceramic. The graph in Fig. 6 shows this once again. Fig. 6 (left) shows the characteristic heating behaviour

<sup>1</sup> For interpretation of color mentioned in this Table 1 the reader is referred to the web version of the article.



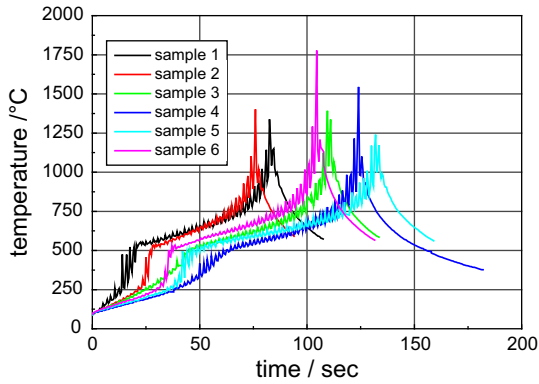


Fig. 5. Heating behaviour of Al<sub>2</sub>O<sub>3</sub> ceramics at a diode laser power of 36.25 W/mm<sup>2</sup>.

for Al<sub>2</sub>O<sub>3</sub> ceramics with and without filler in the joining seam. The energy flux density of the irradiated laser power was 32.42 W/mm<sup>2</sup>. While the energy absorbed in the ceramic body is insufficient to heat the specimen above 500 °C, with filler applied, the temperature rises even above 500 °C, reaching the transition temperature characteristic of Al<sub>2</sub>O<sub>3</sub> of approx. 900 °C above which the intensity of laser–ceramic interaction increases exponentially.

This applies analogously to ZrO<sub>2</sub> ceramics as shown in Fig. 6. The irradiated energy flux density was 6.74 W/mm<sup>2</sup>. As the energy required for defect generation in ZrO<sub>2</sub> is lower than for Al<sub>2</sub>O<sub>3</sub>, the (lower) irradiated energy is sufficient to heat the ceramic even without filler up to the range of the transition temperature of approx. 850 °C. With filler added, heating is expectedly more intensive.

These results are also reflected in the values obtained for the temperature-dependent absorption with the aid of the dual Ulbricht spheres (Fig. 7). The measurement presented here was made during the cooling process of a ZrO<sub>2</sub> ceramic specimen heated up to 950 °C by laser radiation.

The brazing filler used for joining was examined for its composition (after synthesis) by means of X-ray fluorescence analysis (XRF) as well as mass spectrometry with inductively coupled plasma (ICP) (*Inductively Coupled Plasma Mass Spectrometry, ICPMS*) at the RWTH Aachen/GHI. The oxide proportions of the synthesized glass are listed in Table 2, with the proportion being calculated as a difference from 100% in the case of B<sub>2</sub>O<sub>3</sub>.

Measurements of the expansion coefficient have yielded a value of  $\alpha_{600^\circ\text{C}} = 7.4 \times 10^{-6} \text{ K}^{-1}$ , which demonstrates an acceptable difference to the values of the ceramics to be joined.

Optimization of the joining technology relies on the knowledge of the temperature-dependent viscosity of glass fillers. The viscosity of glasses strongly depends on temperature. The glasses have a viscosity of 10<sup>18</sup> Pa s at room temperature. To characterize viscosity as a function of temperature, it is common to determine what is

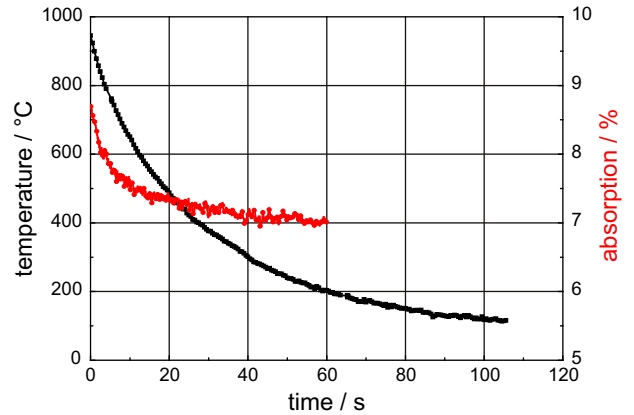


Fig. 7. Temperature and absorption progress of a ZrO<sub>2</sub> ceramic during cooling.

Table 2  
Oxidic composition of the glass filler.

Oxide	Quantity (wt.%)
SiO <sub>2</sub>	11.30
B <sub>2</sub> O <sub>3</sub>	25.30
Al <sub>2</sub> O <sub>3</sub>	19.40
BaO	9.10
SrO	29.70
La <sub>2</sub> O <sub>3</sub>	3.50

termed as viscosity fixed points of a glass. One of these points is e.g. the flow point of a glass which is characterized by a viscosity of 10<sup>4</sup> Pa s. Further states relevant and characteristic in practice are those that can be described by the softening, sphere, half ball and flow temperatures. These are determined using a heating microscope.

The standardized measuring method in accordance with DIN 51730 assigns the aforementioned temperatures to a defined change of shape that is evaluated relative to the initial shape. Whereas the first changes of the investigated cubic geometry are assigned to the softening temperature, the shapes of a sphere or a half ball are relevant to the temperature points of the same name. The flow temperature is, by definition, the temperature at which the body has only one third of its height at half ball temperature. However, no exact viscosity points can be assigned to these temperatures. The characteristic temperatures of the filler used here were measured by means of the heating microscope (GHI/RWTH Aachen).

Since laser joining is a fast process with common process times in the range of seconds to minutes, precise process control is crucial for the achievable seam quality. The following sequential

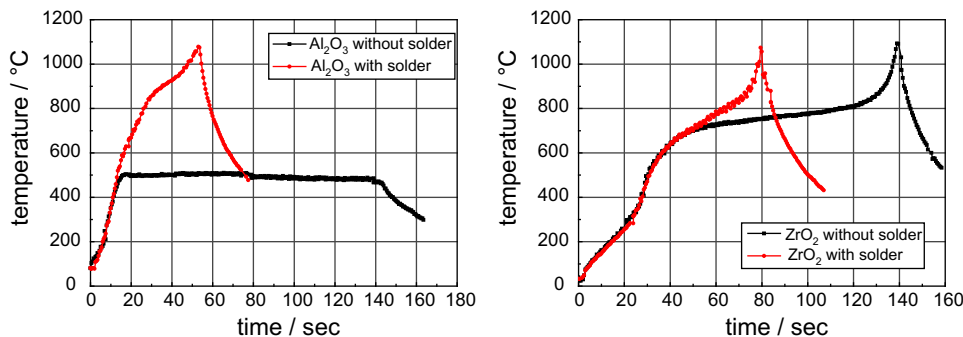
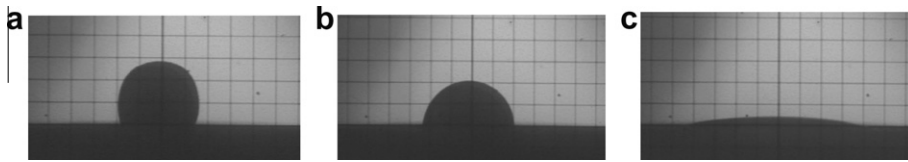
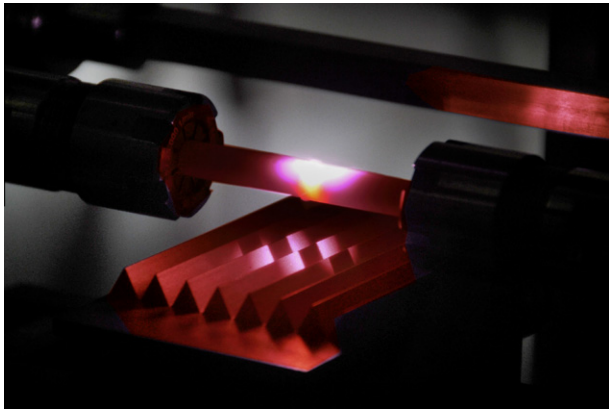


Fig. 6. Heating behaviour of Al<sub>2</sub>O<sub>3</sub> – (left) and ZrO<sub>2</sub> ceramics (right) under diode laser radiation.



**Fig. 8.** Photos of the shaped filler glass body in the heating microscope: (a) sphere temperature 807 °C (left), (b) half ball temperature 824 °C (center), (c) flow temperature 1007 °C (right).



**Fig. 9.** In-line image of laser joining process.

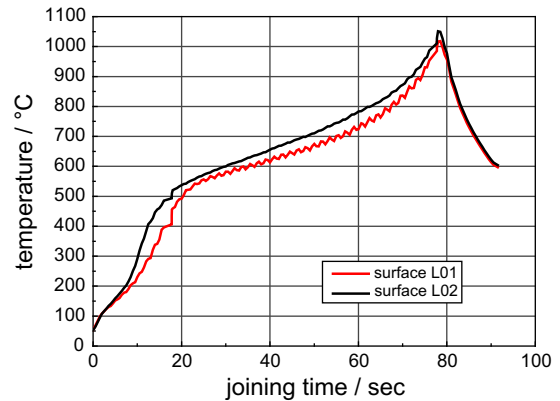


**Fig. 11.** Time-dependent heating of the ceramic surface in the immediate vicinity of the joining seam.

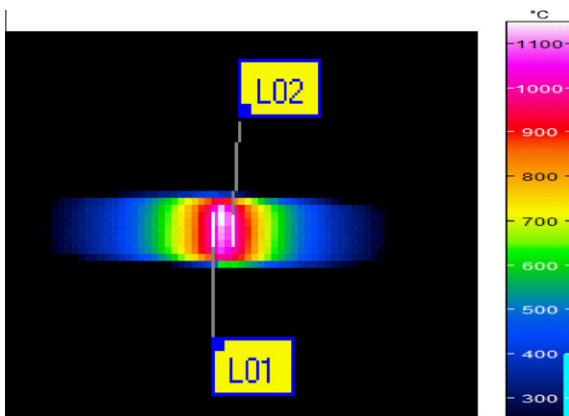


**Fig. 10.** Positions (L01, L02) for measurement of the ceramic surface temperature.



**Fig. 12.** Joined Al<sub>2</sub>O<sub>3</sub> ceramic.

substeps are realized during irradiation time: heating of the ceramic in the area of the joining seam as well as heating of the filler, filler melting, joining of the partners by the liquid glass phase (wetting) as well as the targeted seeping of a minute quantity of glass phase from the joining gap to cover the seam area on the outside. The crucial factor is optimized temperature control. As shown in Fig. 8, the melting temperature of the filler used here is 1007 °C. Starting from this, a maximum process temperature for joining the ceramic parts is defined. This temperature is above the melting limit of the glass filler and, at the same time, ensures optimal viscosity of the glass for laser processing as well as sufficient wetting of the joining partner by the glass melt.

In the case of the Al<sub>2</sub>O<sub>3</sub> ceramics investigated, this temperature is in the range of 1050 ± 20 °C. It is reached by a laser energy of 32.42 W/mm<sup>2</sup> applied to the specimen surface within an adequate time for the laser process. Fig. 9 shows a snapshot of the laser pro-

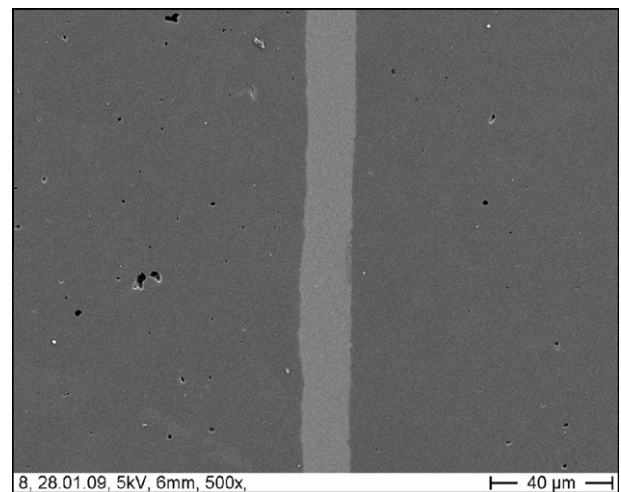


**Fig. 13.** Laser-joined seam.

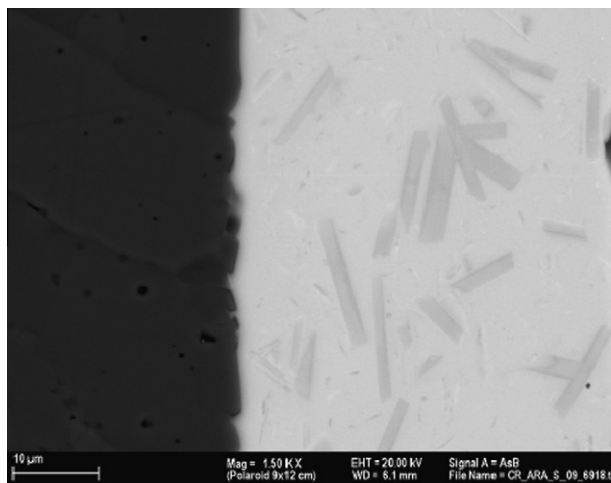


**Fig. 14.** Crystal formation in furnace atmosphere at the contact point between filler and ceramic.

cess when the ceramic surface has reached the maximum joining temperature. An absorber below the exposed sample discharges the scattered laser power.

An infrared camera is used during the joining process to take a transient image of the surface temperature of the ceramic to be joined. In order to control the laser process, local temperature measuring points are selected from the ceramic surface temperature in the immediate vicinity of the joining seam (cf. Fig. 10). Fig. 11 shows the ceramic temperature curve over time for an  $\text{Al}_2\text{O}_3$  sample.

When the aforementioned laser power is applied, the laser joining process is completed within 80 s. The homogeneous heating of both joining partners in the vicinity of the joining seam is a necessary condition for equal wetting by the glass phase of the areas to be joined. The joint achieved between the  $\text{Al}_2\text{O}_3$  partners with the filler used here is glassy, transparent and largely free from gas inclusions (Fig. 12).

SEM investigations of the joint (Fig. 13) exhibited very good filler adhesion to the joined areas of the  $\text{Al}_2\text{O}_3$  ceramic partners. The seam widths measured were below  $20\ \mu\text{m}$ . The boundary region of glass filler and ceramic showed no formation of intermediate layers.

Since the filler used is not reactive and its stable equilibrium phases have already been reached in the upstream furnace process during glass synthesis, there are apparently no further chemical changes in the joining zone during the short laser joining phase. The assumption that the time factor is crucial is also supported by the research of [12]. When the same filler was pre-sintered on the ceramic in the furnace and subsequently laser-joined, the formation of stable needle-shaped crystals in the glass phase was observed only in the joining gap (Fig. 14). EDS analysis of the crystals revealed the presence of Ba, Sr, Al, Si and O in slightly modified concentrations as compared with the surrounding glass matrix.

The four-point bending strength test revealed that the breakage resulted exclusively from failure in the braze joint between the ceramic partners.

Investigations of the structure in the laser-irradiated joint region demonstrated that, during brazing, no macroscopic cracks have been induced in the adjacent ceramic. Using optimized glass systems, it was possible to achieve average strengths of 158 MPa for the  $\text{Al}_2\text{O}_3$ – $\text{Al}_2\text{O}_3$  joints and of 190 MPa for the  $\text{ZrO}_2$ – $\text{ZrO}_2$  joints. The tested series included up to 20 specimens. The standard deviation for the joined  $\text{Al}_2\text{O}_3$  and  $\text{ZrO}_2$  specimens was 34 MPa and 31 MPa, respectively.

#### 4. Conclusions

The results achieved showed that by using a glass filler the selected oxide ceramics ( $\text{Al}_2\text{O}_3$ ,  $\text{ZrO}_2$ ) can be positively bonded at temperatures above  $1000\ ^\circ\text{C}$ , at the specific wavelengths of a diode laser (808–1010 nm). Besides the typical laser parameters, the factors considered in the optimization of the laser-induced joining process were the process-relevant properties of the ceramic (emissivity, optical properties and heating behaviour at defined laser power) and of the filler used (absorption of laser radiation, softening characteristics and expansion coefficient). The glass–ceramic joints produced are free from gas inclusions and macroscopic defects and exhibit a homogenous structure. The average strength values achieved were 158 MPa for the  $\text{Al}_2\text{O}_3$  system and 190 MPa for the  $\text{ZrO}_2$  system, respectively.

Experiments on joint lifetimes under defined conditions are planned for the near future. Process times in the range of seconds to minutes and the localized heating up of the joining partners by means of a laser beam are the prerequisites for producing also complex composite geometries by laser joining. Further experimental research in this field is planned.

#### Acknowledgements

Part of the published results was achieved by research under the joint project “Joining of ceramic components by laser brazing – New simulation tools develop an innovative technology” (Fund No. 03X0507F of the Federal Ministry of Education and Research). The authors gratefully acknowledge the financial support by the Federal Ministry of Education and Research.

#### References

- [1] A Technology Roadmap for Generation IV Nuclear Energy Systems, Issued by the US DOE Nuclear Energy Research Advisory Committee and the Generation IV International Forum, December 2002. <<http://gif.inel.gov/roadmap>>.
- [2] T.E. Lipman, What Will Power the Hydrogen Economy? Present and Future Sources of Hydrogen Energy, UCD-ITS-RR-04-10, Institute of Transportation Studies, University of California, Berkeley.
- [3] T. Schulenberg, L. Behnke, J. Hofmeister, M. Löwenberg, Was ist Generation IV? Forschungszentrum Karlsruhe, Wissenschaftliche Berichte FZKA 6967, February 2004.
- [4] DFG-Schwerpunktprogramm 1299/DFG Priority Programme 1299: Adaptive Oberflächen für Hochtemperatur-Anwendungen/Adaptive Surfaces for High Temperature Applications (Project: Thermisch stabile keramische Membranen mit integriertem Gassensor für Gasseparation und Detektion von Wasserstoff und Kohlenmonoxid bei hohen Temperaturen).
- [5] F. Heilmann, G. Rixecker, F.-D. Börner, W. Lippmann, A. Hurtado: Laser hybrid brazing of oxide ceramics for high temperature gas sensing applications in (V)HTRs, Jahrestagung der Kernenergetischen Gesellschaft 2009, Dresden.
- [6] M.G. Faga, S. Guicciardi, L. Esposito, A. Bellosi, G. Pezzotti, Advanced Engineering Materials 7 (6) (2005) 535–540.
- [7] W. Lippmann, M. Herrmann, C. Hille, A. Hurtado, A.-M. Reinecke, R. Wolf, Sonderheft cfi-Berichte der Deutschen Keramischen Gesellschaft 85 (Heft 13) (2008) 60–64.
- [8] S. Kasch, G. Köhler, H. Müller, S. Wächter, Prozess- und funktionsangepasstes Laserstrahllöten mit Glaslot für Sensor- und Displayanwendungen, in DV5, vol. 243, 2007, pp. 201–204.
- [9] G. Köhler, H. Müller, S. Kasch, Laserstrahlfügen von  $\text{Al}_2\text{O}_3$ –Keramik mittels Glaslot, in Fortschrittberichte VDI, Nr. 347, 1995, pp. 84–89.
- [10] S. Kasch, G. Köhler, H. Müller, R. Daferner, D. Mund, H. Paschke, Application of laser-beam soldering for joining ceramics and glasses by using solder glasses, in Tagungsband “Joining’97”, 1997, pp. 1–4.
- [11] W. Lippmann u.a., Fortschrittsberichte der Deutschen Keramischen Gesellschaft 21 (1) (2007) 143.
- [12] F. Heilmann, Dreidimensionales Laserhybridlöten zum dauerhaften Fügen gleicher und ungleicher Oxidkeramiken, Diss., TU Dresden, 2009.
- [13] F.-D. Börner, W. Lippmann, A. Hurtado, Laserfügen von Oxidkeramiken, Jahrestagung der Deutschen Keramischen Gesellschaft, 2009, Aachen.
- [14] P.-L. Lo, L.-S. Chang, Y.-F. Lu, Ceramics International 35 (8) (2009) 3091–3095.
- [15] M.L. Shalz, B.J. Dagleish, A.P. Tomsia, A.M. Glaeser, Journal of Materials Science 28 (1) (1993) 1673–1684.
- [16] Norbert Schuster, Valentin Kolobrodov, Infrarotthermographie, Wiley-VCH, Berlin, 2000 (ISBN 3-527-40130-X).

- [17] F.v. Alvensleben, C.W. Byun, C. Dannat, *Keramische Zeitschrift* 44 (1997) 446–449.
- [18] J. Manara, R. Caps, F. Raether, J. Fricke, *Optics Communications* 168 (1999) 237–250.
- [19] O.G. Tsarkova, S.V. Garnov, V.I. Konov, E.N. Lubnin, F. Dausinger, *SPIE* 3618 (1999) 198–207.
- [20] P.A. Skiba, V.P. Volkov, K. Predko, V.P. Veiko, *Optical Engineering* 33 (11) (1999) 3572–3577.
- [21] D. Ouyang, C. Mo, I. Zhang, *NanoStructured Materials* 7 (5) (1996) 573–578.
- [22] Z. Zhang, M.F. Modest, *Journal of Heat Transfer* 120 (2) (1998) 322–327.